Trends in Biochemical Sciences

CellPress

Review

Chemistry and Biology of Self-Cleaving Ribozymes

Randi M. Jimenez,[1] Julio A. Polanco,[1] and Andrej Lupták[1,2,3,*]

Self-cleaving ribozymes were discovered 30 years ago, but their biological distribution and catalytic mechanisms are only beginning to be defined. Each ribozyme family is defined by a distinct structure, with unique active sites accelerating the same transesterification reaction across the families. Biochemical studies show that general acid-base catalysis is the most common mechanism of self-cleavage, but metal ions and metabolites can be used as cofactors. Ribozymes have been discovered in highly diverse genomic contexts throughout nature, from viroids to vertebrates. Their biological roles include self-scission during rolling-circle replication of RNA genomes, co-transcriptional processing of retrotransposons, and metabolite-dependent gene expression regulation in bacteria. Other examples, including highly conserved mammalian ribozymes, suggest that many new biological roles are yet to be discovered.

Trends

Self-cleaving ribozymes are distributed throughout all branches of life. Currently, there are nine distinct structural motifs that promote self-scission in nature.

The six self-cleaving ribozymes that have been investigated mechanistically all appear to use a general acid-base mechanism for catalysis. Magnesium, or another divalent metal ion, is largely used to stabilize the tertiary structures of these ribozymes.

The broad distribution of self-cleaving ribozymes suggests several biological roles. The known functions include RNA processing during rolling-circle replication of single-stranded subviral pathogens and satellites, co-transcriptional scission of retrotransposons, and (pre-)mRNA cleavage.

Genomic locations of these ribozymes suggest that they affect many other biological processes, some of which may not be directly associated with RNA scission.

Guiding Principles for Ribozyme Exploration

Small nucleolytic ribozymes carry out site-specific phosphodiester scission without the need for protein chaperones or enzymes. A growing number of ribozyme families are found in nature, including hairpin, hammerhead, **hepatitis delta virus (HDV)-like** (see Glossary), **glucosamine-6-phosphate synthase** (glmS), *Neurospora* Varkud satellite (VS), twister, the recently discovered twister sister, pistol, and hatchet motifs. All rely on a combination of catalytic strategies to complete self-scission in an active site formed by the secondary and tertiary structures unique to each family. For these ribozymes, cleavage involves a nucleophilic attack by a 2′ oxygen on an adjacent phosphodiester bond, yielding a 2′-3′ cyclic phosphate and a 5′-hydroxyl product (Figure 1). Crystal structures have been essential to illuminate how functional groups participate in the catalytic mechanism used by each family of ribozyme. The local electronic environments within the active sites shift pK_a values, allowing nucleobases and cofactors to participate in general acid-base catalysis. Despite the plethora of information regarding their genomic distributions, structures, and mechanisms, the biological roles of the three most widespread families (hammerhead, HDV-like, and twister) remain largely elusive. The study of small ribozymes has provided a platform for discovering new catalytic RNAs and new roles for **noncoding RNA** (ncRNA), as well as aiding in the design of new molecules for synthetic biology. Here, we summarize the recent mechanistic findings of the six best-described types of self-cleaving ribozyme and discuss their potential impact on the surrounding transcripts. The discovery of three new types of self-cleaving ribozyme earlier this year (2015) suggests that there are more catalytic RNAs with new biological functions to be uncovered.

Hepatitis Delta Virus Family of Ribozymes

The HDV life cycle depends on coinfection with hepatitis B virus (HBV) [1] and relies on host cellular machinery for rolling-circle replication of its single-stranded RNA genome (Figure 2A) [2]. The HDV genome encodes two related but distinct ribozymes that were first discovered through their function in processing concatemeric copies of the viral RNA genome during rolling-circle transcription (Figure 2A) [3]. More recently, this ribozyme motif was discovered in the human

[1]Department of Molecular Biology and Biochemistry, University of California, Irvine, CA, USA
[2]Department of Pharmaceutical Sciences, University of California, Irvine, CA, USA
[3]Department of Chemistry, University of California, Irvine, CA, USA

*Correspondence: aluptak@uci.edu (A. Lupták).

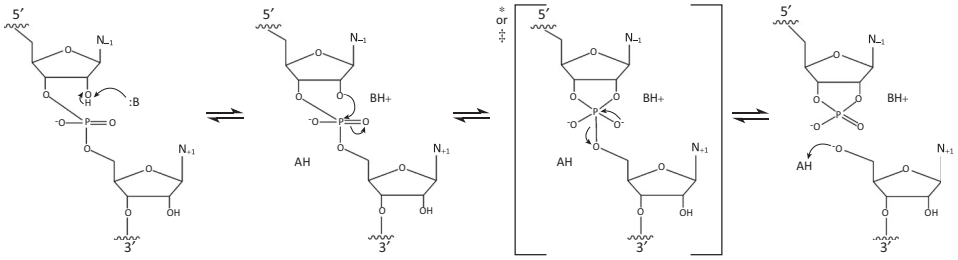

Figure 1. Mechanism of RNA Self-Scission. A general acid-base catalysis involves a general base, which deprotonates the 2′ hydroxyl of the nucleophile, positioned in-line with the 5′ O leaving group. The transesterification proceeds via a phosphorane transition state or intermediate, depending on whether it is stabilized, yielding a 2′-3′ cyclic phosphate in the upstream nucleotide and an oxyanion on the downstream nucleotide. The leaving group is protonated by a general base. The small self-cleaving ribozymes described here use a variety of chemical groups to facilitate this process (Table 1, main text).

genome using *in vitro* selection from a genomic library; sequence analysis showed that it is highly conserved in mammals [4]. When its nested double-pseudoknot secondary structure was used to identify the motif in other genomes (Box 1), the family of HDV-like ribozymes was found to exist in nearly all branches of life [5]. These HDV-like ribozymes often map to the 5′ **untranslated region** (UTR) of autonomous [**long interspersed nuclear elements** (LINEs)] retrotransposons, pointing to a role in the processing of retrotransposons (Figure 2B). Expression analysis and 5′ processing studies support a model in which HDV-like ribozymes function at several stages of non-**long terminal repeat** (non-LTR) retrotransposition [6–8]. Besides processing the 5′ end of the transposon RNA out of the parent transcript, ribozymes may be promoting the translation of the open reading frame of the retroelement [5] and facilitating the insertion of the retrotransposon into a new DNA locus. In support of this idea, an RNA 5′-hydroxyl, such as would result from ribozyme self-cleavage, increases efficiency of R2 reverse transcriptase template switching, completing the R2 LINE retrotransposition cycle [9,10].

Further biological roles of these ribozymes suggest that their activity: (i) is regulated; (ii) affects the surrounding transcript; and, remarkably, (iii) is associated with a phenotype in humans. In the mosquito *Anopheles gambiae*, expression and self-scission analyses revealed that both the *in vivo* levels and the extent of self-cleavage vary by sex and life stage [5], suggesting environmental sensitivity and regulation. The HDV-like ribozyme found in an intron of the cytoplasmic polyadenylation element binding protein 3 (*CPEB3*) gene is highly conserved in mammals [4], and humans homozygous for a **single nucleotide polymorphism** (SNP) known to affect *CPEB3* ribozyme activity show differences in episodic memory [11]. Other HDV-like ribozymes are located at unrelated genomic loci in both coding and noncoding transcripts, suggesting multiple biological functions. HDV-like ribozymes have fast self-cleavage kinetics and a remarkably stable structure, demonstrating activity in up to 18 M formamide [12,13]; therefore, some of the cellular functions may be related to stabilizing the 5′ termini of the cleaved transcripts and protecting them from degradation by exonucleases.

The HDV ribozyme secondary structure comprises five helical regions (P1.1, P1, P2, P3, and P4) forming two coaxial stacks (P1 and P1.1 stack on P4, and P2 stacks on P3) that are joined by single-stranded regions (J1/2, L3, and J4/2) (Figure 3A). There are six conserved nucleotides fulfilling functional or structural roles in the active site. The ribozyme exists naturally in a minimal (lacking P4) or extended (extension of J1/2 and P4) form. Crystal structures of the genomic HDV ribozymes revealed that the secondary structure forms a nested double-pseudoknot (Figure 3A) and the active site is buried in the junction of P1, P1.1, and P3 [14–16]. The protonated form of C_{75} is thought to be stabilized through interactions with the scissile phosphate [16] and may

Glossary

Cofactor: a chemical compound that is directly involved in the catalytic mechanism by a catalytic macromolecule. To our knowledge, the HDV and *glmS* ribozymes are the only self-cleaving ribozymes that utilize cofactors (Mg^{2+} and glucosamine 6-phosphate, respectively) as part of their reaction mechanism.

General acid-general base catalysis: a reaction where a certain chemical group is involved in proton transfer. In most cases, a nucleobase fulfills the role of general base by abstracting a proton from the 2′ OH of the attacking group and another nucleobase acts as general acid by protonating the 5′ oxyanion leaving group (Figure 1, main text).

Glucosamine-6-phosphate synthase (glmS): also known as glutamine-fructose-6-phosphate transaminase. The protein encoded by the *glmS* gene has been shown to participate in the peptidoglycan synthesis pathway for bacterial cell wall synthesis. The substrates for the aminotransferase reaction catalyzed by the glmS enzyme are L-glutamine and D-fructose 6-phosphate and the product is D-glucosamine 6-phosphate. The glmS enzyme is activated upon post-translational modifications by protein factors, and the enzyme activity is inhibited by glucose-6-phosphate.

Hepatitis Delta Virus (HDV): a hepatitis B virus (HBV) helper virus, HDV has a small circular single-stranded RNA genome that encodes one protein, the delta antigen. Both the sense and antisense genomes of the virus encode a self-cleaving ribozyme of the same secondary structure, but have a different sequence.

Hepatitis delta virus-like (HDV-like): refers to the structural similarities between the HDV ribozyme to that of a ribozyme identified within the genome of an organism. One example includes the HDV-like ribozyme encoded within the cytoplasmic polyadenylation element binding protein 3 (*CPEB3*) gene in mammals.

Long interspersed nuclear element (LINE): a type of eukaryotic non-LTR transposon capable of propagation through an RNA intermediate. LINE elements are repetitive in sequence, can be as

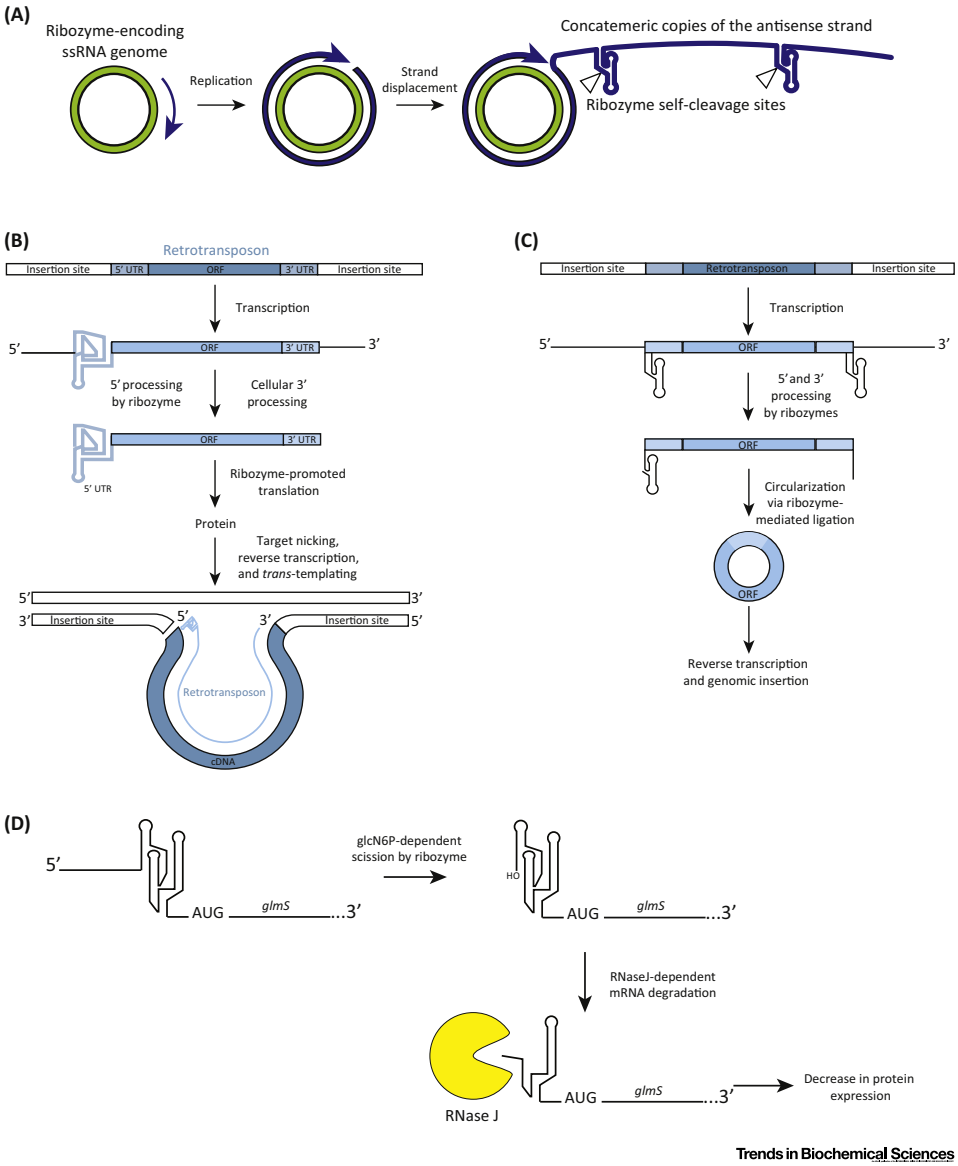

Figure 2. Roles of Self-Cleaving Ribozymes in Different Biological Systems. (A) Most instances of self-cleaving ribozymes found in (sub-)viral genomes are involved in replication. During rolling-circle replication of a single-stranded (ss) RNA genome, concatemeric copies of the opposite polarity are generated. The self-cleavage activity of ribozymes generates unit-length copies that must be circularized and replicated to complete the cycle. (B) Retrotransposon-associated hepatitis delta virus (HDV)-like ribozymes liberate the 5′ end of the retroelement from the full-length transcript. The ribozyme structure in the 5′ untranslated region (UTR) promotes translation of the downstream open reading frame (ORF). The protein produced is necessary for target nicking, reverse transcription, and genomic insertion. Further, the HDV-like ribozyme on the 5′ end of the RNA promotes the template switching necessary to complete genomic insertion of the autonomous (long interspersed nuclear elements; LINEs) element. (C) Hammerhead ribozymes mapping to nonautonomous retrotransposons (short interspersed nuclear elements; SINEs) serve to mobilize the retroelement. Complementarity of the 5′ and 3′ ends facilitates ribozyme self-ligation, resulting in circularization of the RNA; this feature enhances the reverse transcription and genomic insertion processes that complete the retrotransposition cycle. (D) The glucosamine-6-phosphate synthase (*glmS*) ribozyme is located in the 5′ UTR of the *glmS* gene, encoding the glutamine-fructose-6-phosphate aminotransferase enzyme responsible for generating glucosamine 6-phosphate (glcN6P), necessary for bacterial cell wall synthesis. The ribozyme requires glcN6P as a cofactor for catalysis. The resulting 5′-hydroxyl makes the processed transcript a substrate for the 5′-3′ exonuclease RNase J. Therefore, the *glmS* ribozyme is a riboswitch that turns off glcN6P synthase expression in response to glcN6P.

long as a few thousand base pairs, and encode the necessary proteins required for autonomous retrotransposition.

Long terminal repeat (LTR): the repetitive sequence found at termini of a retroviral genome that encodes specific proteins necessary for infection and propagation. Non-long terminal repeats (non-LTRs) only replicate within a genome and are defined as retrotransposable elements that prime their cDNA from nicked target DNA.

Noncoding RNAs (ncRNAs): transcribed RNAs that are not translated. Many ncRNAs have been shown to participate in RNA processing and assembly in ribonucleoprotein complexes. These include tRNAs, rRNAs and small nuclear RNAs.

Penelope-like elements (PLEs): a distinct family of retrotransposons identified within a large number of eukaryotic genomes. PLEs are classified by two direct repeats flanking a single open reading frame that encodes reverse transcriptase proteins, an endonuclease, and sometimes retains introns.

Short interspersed nuclear element (SINE): RNA fragments that are a few hundred nucleotides in length and usually comprise tandem repeats. These RNA transcripts are not translated, but have been shown to be propagated by enzymes encoded by LINEs.

Single nucleotide polymorphism (SNP): a type of genetic variation that is observed within a population that shares the same genomic sequence. This variation occurs at a single nucleotide and at the same genomic location.

Transition state stabilization: a transition state is a high-energy species formed during the course of a chemical reaction. The stabilization of the transition state accelerates the chemical reaction. During ribozyme self-cleavage, phosphorane forms the transition state, which can be a true intermediate if it is stabilized through hydrogen bonding of one of the nonbridging phosphates or by a counter ion (e.g., a metal ion).

Untranslated region (UTR): a region of an mRNA molecule that corresponds to the sequence before the translation start codon and after the translation termination codon. UTRs are important for regulation of the transcript.

Box 1. Structural Conservation in Ribozymes

As a single-stranded nucleic acid polymer, RNA is capable of folding into diverse and intricate secondary and tertiary structures. The basis of RNA secondary structure is its capacity for base pairing of antiparallel strands into helices within a single molecule. Since base pairing only dictates that complementary nucleotides are recognized through standard Watson–Crick or wobble interactions, the actual sequence of a helix need not be conserved, as long as the interacting nucleotides are complementary (e.g., within a helix, a C–G base pair serves the same function as an A–U). In general, structures of RNAs are dominated by helical segments, which are defined on the sequence level by base-pair covariation. Therefore, unlike protein structures, which typically share conserved sequences, RNA motifs are typically not conserved at a sequence level, but are dominated by segments of sequence that covary with their pairing partners and, thus, are hard to identify through sequence alignments. Currently, bioinformatics methods identify patterns of covariation across predicted secondary structures, and these patterns are an indicator of RNA structural conservation, leading to the discovery of new functional RNA families [102].

Tertiary structure is the global architecture of a single molecule formed by the combination of contacts outside of helical base pairing through hydrogen bonding, base stacking, and other specific interactions. An RNA structural motif is conserved if it preserves the secondary and tertiary structure, although not necessarily the topology, of an RNA. Here, topology refers to the order that the individual structural elements appear in the motif. For example, the Y-shaped hammerhead ribozyme (Figure 3B, main text) can connect to the flanking transcript via the termini of any of its three helices, giving rise to three different topologies, but the same tertiary structure.

Viroids: short (~250–~450 nucleotide) circular single-stranded RNA infectious pathogens found mostly in plants. Also known as subviral pathogens, they are replicated through rolling-circle replication by RNA polymerase II.
Virusoids: similar to viroids, these are circular single-stranded RNA pathogens that depend on viruses for rolling-circle replication and encapsulation. They are classified as subviral particles and satellites.

interact electrostatically with the metal ion bound in the active site [17]. Divalent metals have a profound impact on catalysis and recent evidence reveals a Mg^{2+} ion in a metal-binding pocket in the ribozyme active site [16,18].

The proposed mechanism of catalysis suggests that HDV ribozymes are multichannel, using different strategies in the presence and absence of divalent metal ions. In one scenario, the protonated form of C_{75} donates a proton to the 5′-O of G_1 [19]. The HDV-like ribozymes are metalloenzymes under biological conditions with the divalent metal cation thought to stabilize the developing negative charge on the 2′ nucleophile [18], facilitating deprotonation by a general base, likely a hydroxide ion, and also potentially stabilizing the pentavalent phosphorane transition state [20]. There is little metal ion specificity and catalysis can proceed in high concentrations of monovalent cations alone [21]. In the absence of divalent cations, the dramatic shift in pK_a of the catalytic nucleobase C_{75} may be sufficient to stabilize the negatively charged nucleophile and general acid-base catalysis proceeds without mediation by a divalent metal cation [22,23]. Even though HDV ribozymes were the first to have a general acid-base mechanism proposed [20], efficient catalysis by HDV and HDV-like ribozymes appears to require both a divalent metal ion and an active-site cytosine acting as a general acid (Table 1). This mechanism turns out to be unique among natural self-cleaving ribozymes, because the other motifs described in this review all appear to only use nucleotides for catalysis (Table 1).

Table 1. Common Themes in Self-Cleavage Mechanisms

Ribozyme Family	Deprotonates 2′ Nucleophile	Proposed Transition State Stabilization	Protonates 5′ Leaving Group	Refs
HDV	Hydrated Mg^{2+}	Mg^{2+} as Lewis acid	C_{75}	[14,16]
Hammerhead	G_{12}	?	G_8	[43]
Hairpin	G_8	G_8	A_{38}	[52]
Neurospora VS	G_{638}	G_{638}	A_{756}	[60]
glmS	G_{40}	GlcN6P	GlcN6P	[78,79]
Twister (Osa-1-4)	G_{45}	G_{45}	A_7?	[84]
(*env22*)	C_{46}, A_{47}?	A_{47}, G_{48}	?	[85]
(env)	G_{62}	A_{63}	?	[86]

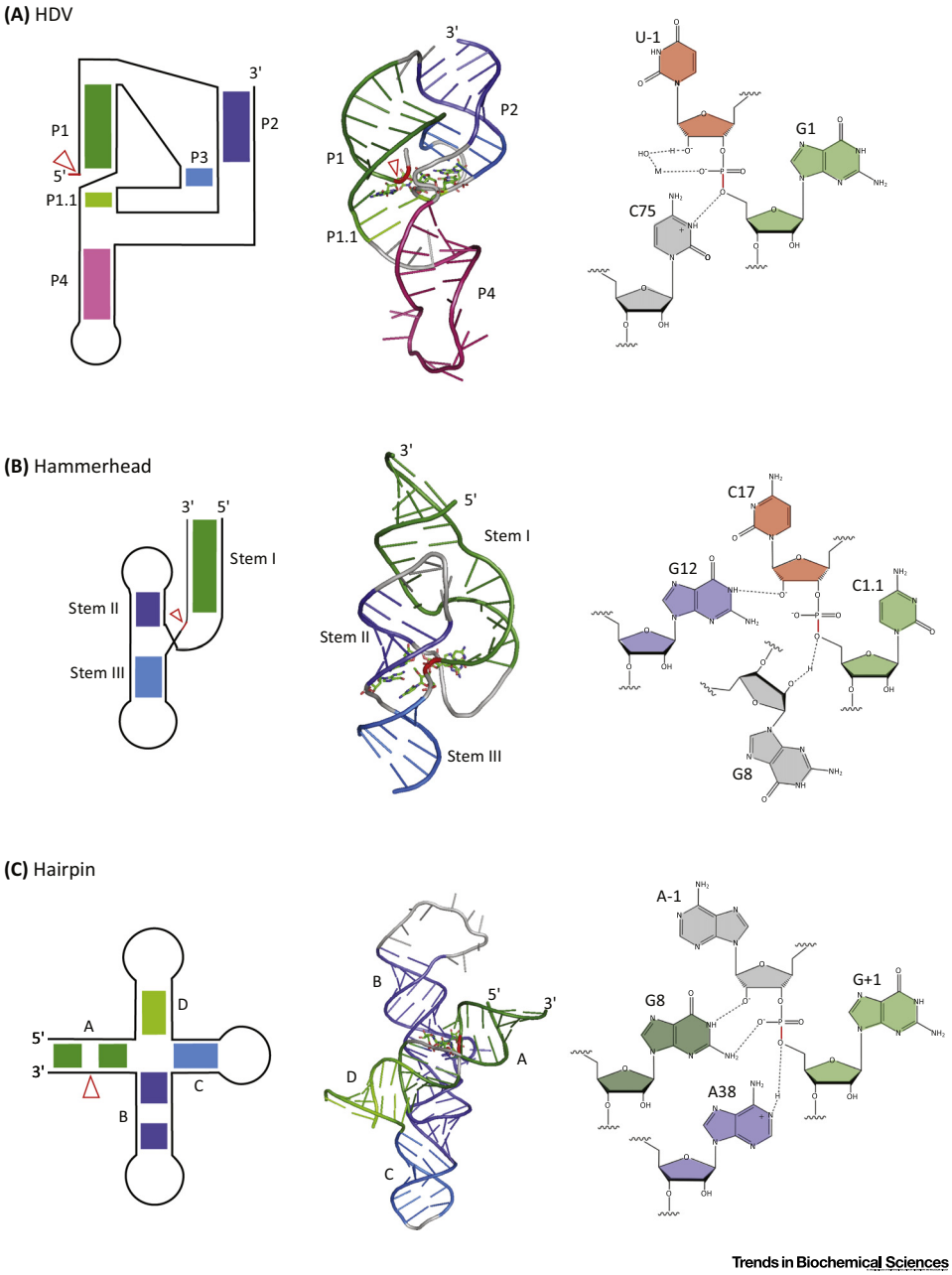

Trends in Biochemical Sciences

Figure 3. Overview of Self-Cleaving Ribozymes: Structural Features and Proposed Cleavage Mechanisms.
The secondary structures of the (A) hepatitis delta virus (HDV)-like, (B) hammerhead, (C) hairpin, (D) *Neurospora* Varkud satellite (VS), (E) glucosamine-6-phosphate synthase (*glmS*), and (F) twister ribozymes are shown in the left column and labeled as they appear in current literature. Typically, the helical segments are numbered as 'paired' elements (P1, P2, etc.), by Roman numerals, or in alphabetical order in a 5′ to 3′ direction as they appear in the first example of a given motif. Paired regions corresponding to pseudoknots are designated PK or simply as paired elements. The corresponding crystal structures for each ribozyme are shown in the middle column with colored helices to emphasize helical stacks and pseudoknots. The site of scission is pointed out by the red arrowheads in the secondary structures and highlighted in red in the respective crystal structures. A model of the cleavage site for each ribozyme is shown in the right column, which illustrates interactions that promote the cleavage event. Nucleobases flanking the scissile phosphate are splayed apart, which promotes the in-line orientation necessary to accomplish cleavage. The scissile bond is shown in red. Interactions proposed to stabilize the transition state of the reaction are shown for all ribozymes. Note that all cleavage sites, with the exception of the HDV-like ribozyme, which requires a hydrated metal (M), have a guanosine residue that participates as a proposed general base in the general acid-base reaction mechanism. The *glmS* ribozyme requires glucosamine-6-phosphate (glcN6P) as a cofactor necessary for catalysis. For the twister ribozyme, a hypothetical interaction (dashed red line) between N3 of A_7 and the scissile phosphate suggests that A_7 acts as the general acid during self-cleavage. Protein Data Bank IDs are 3ZD5 (A), ISJ3 (B), IM5K (C), 2NZ4(D), and 4QJH (E).

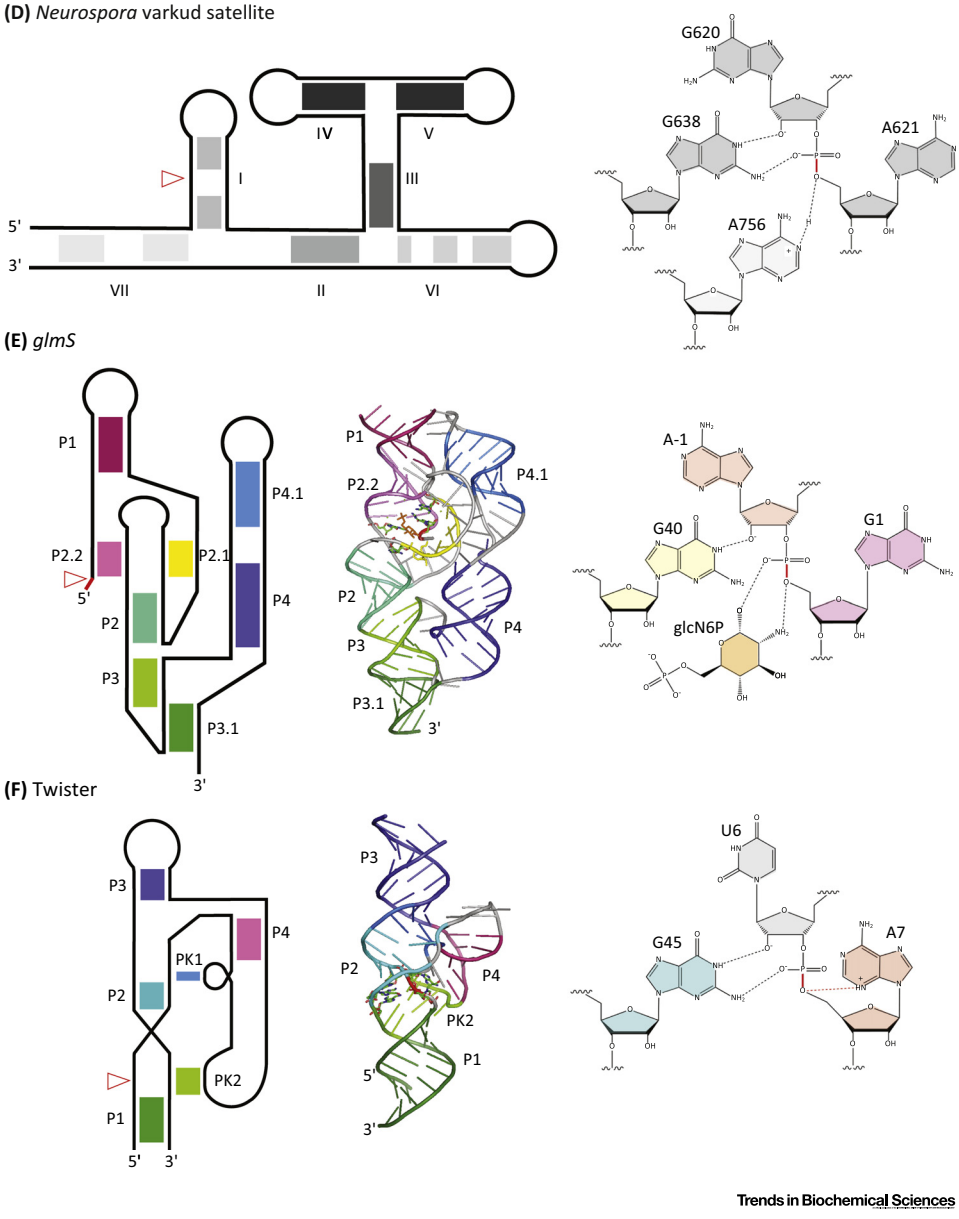

Figure 3. (continued)

Hammerhead Ribozyme

The hammerhead ribozyme (HHR) was originally discovered in **viroids** and **virusoids**, where it functions in the processing of rolling-circle transcripts (Figure 2A) [24–26]. Over the two decades following its discovery, isolated instances were found in various newt species [27], cave crickets [28], and the human blood fluke *Schistosoma mansoni* [29]. HHRs found in the genomes of various schistosomes map to **short interspersed element-like** (SINE) retrotransposable elements (Figure 2C) [29,30]. The conservation of these SINE-associated HHRs suggests vertical transmission from a common ancestor of schistosomes. The HHR is perhaps the most widespread ribozyme family, having been found across all domains of life [27,29,31–35]. Most eukaryotic occurrences map to satellite transcripts and retroelements; however, a conserved

group in amniotes map to the introns of specific genes [32,33,36]. This conservation in introns implicates a role for these ribozymes in pre-mRNA processing. The ribozyme has also been found bisected into two fragments hundreds of nucleotides apart between the stop codon and the polyadenylation signal of mouse C-type lectin type II (*Clec2*) and some mammalian *Clec2-like* genes [37]. It seems that the mechanism of ribozyme phosphodiester scission may have been adapted to introduce diversity in gene expression and more complex genetic controls, but more research is needed to decipher the potential role of HHRs in intron cleavage and pre-mRNA processing. The efficient self-scission of HHRs *in vitro* and *in vivo* suggests that the activity is central to their biological significance.

The HHR secondary structure comprises three helices (stems I, II, and III) branching from a catalytic core containing 15 nucleotides essential to catalysis (Figure 3B). The ribozyme exists naturally in three circularly permuted topologies (types I, II, and III), defined by the helix connecting it to the surrounding transcript (Box 1). The HHR was the first ribozyme to have its crystal structure solved [38,39], revealing the core trapped in an open or precatalytic state that would require significant rearrangement to bring the essential residues into position for in-line attack. Subsequent mechanistic and structural data conflicted until the discovery of a distal tertiary contact (between stems I and II) [40,41], which promotes significantly faster cleavage rates, because it stabilizes the catalytically competent conformation of the active site. The global structure of the ribozyme is Y shaped, comprising a coaxial stack of stems III and II that pack next to stem I (Figure 3B), optimally positioning residues implicated in general acid-base catalysis, and for the nucleophile to attack the scissile phosphate [42].

The currently proposed model of catalysis by a HHR involves only nucleotides participating directly in catalysis. Biochemical and crystallographic evidence supports C_{17} nucleophilic attack on the adjacent scissile phosphate of $C_{1.1}$. Invariant residues G_8 and G_{12} serve as a general acid and a general base, respectively [43]. A recent crystal structure revealed three Na^+ cations in the HHR active site, one of which binds to G_{12} and may be involved in stabilizing the negative charge of the deprotonated N1 position [44]. A role for monovalents in perturbing the pK_a of the general base had been suggested previously [45,46]. The N1 of the ionized form of G_{12} is thought to abstract the 2′ hydrogen from the nucleophilic oxygen of C_{17}; the 2′-O is then positioned for in-line attack on the phosphate of $C_{1.1}$ (Figure 3B) [47]. The ribose of G_8 likely hydrogen bonds to the 5′-oxyanion and donates a proton to the leaving group [42,47,48]. The proposed mechanism is unique in that it uses a nucleobase and a ribose, a composition that may be easier to bring into the active site than two nucleobases or exogenous cofactor, and may contribute to the high frequency with which this self-cleaving ribozyme is found in nature.

Hairpin Ribozyme

There are only three known examples of the hairpin ribozyme family, residing in the satellite RNAs of the tobacco ringspot [24], chicory yellow mottle [49], and arabis mosaic [50] viruses. Each occurrence coincides with the appearance of a HHR on the RNA of the opposite strand and together these ribozymes function in processing multimeric RNA during rolling-circle replication of the viral genome (one on the + strand and one on the – strand). The hairpin ribozyme secondary structure comprises four helical stems (A–D) anchored in a four-way junction and forming two coaxial stacks (D stacks on A, and C stacks on B) (Figure 3C). Stems A and B contain internal bulges housing the scissile phosphate (stem A) and nucleotides essential to catalysis, whereas stems C and D provide structural stability and are not necessary for ribozyme activity.

Crystal structures of the hairpin ribozyme have been determined with and without stems C and D, the junction [51] and hinge forms [52], respectively. The structures support biochemical

evidence for the intimate interaction of loops A and B, which form the active site of the ribozyme (Figure 3C) [51–53]. A_{38} and G_8 are optimally positioned to serve as general acid and general base, respectively. G_8 is on the strand opposite of the scissile phosphate in loop A and A_{38} is in loop B. Single molecule studies revealed that the loop–loop interaction is dynamic and oscillates between an antiparallel (active form) and parallel states [54,55].

The highly stabilized extrusion of G_{+1} constrains the riboses of A_{-1} and G_{+1}, respectively, the nucleotides upstream and downstream of the cleavage site, enabling the in-line arrangement of the nucleophile and leaving group [52]. The crystal structure of hairpin enzymes with vanadate, a transition state mimic, points to a role for A_{38} and G_8 as general acid and general base, as well as transition state stabilization by binding the *pro-R* and *pro-S* oxygens of the scissile phosphate, respectively [53]. These roles are supported by functional group modifications and nucleobase substitution experiments [56–59] and appear to exemplify the most general theme in self-scission mechanisms (Table 1).

Neurospora Varkud Satellite Ribozyme

The VS ribozyme is important in replication of a single-stranded RNA satellite found in some strains of *Neurospora* [60]. The secondary structure of the VS ribozyme comprises seven helices (I–VII) that form three three-way junctions (Figure 3D). A kissing loop interaction between stem-loops (SL) I and V [61] facilitates docking of the internal loop of stem I with the internal loop of stem VI, which forms the active site. First predicted based on site-directed mutagenesis and chemical modification analysis [62,63], the interaction involves a conformational change (shift) in SLI that is necessary for ribozyme activity [64–66]. The SLI–SLV interaction facilitates the docking of SLI with SLVI, thereby forming the active site [65,67,68]. The SLI–SLV kissing loop NMR structure has been solved [69–71] and supporting isothermal titration calorimetry experiments demonstrate that the SLI–SLV kissing-loop interaction is a major thermodynamic barrier and, therefore, is likely regulating ribozyme activity [61]. The formation of the SLI–SLV interaction relies upon divalent metal cations; however, there is no evidence for their direct involvement in catalysis.

There is currently no crystal structure solved for the VS ribozyme; however, X-ray scattering experiments reveal that A_{756} (stem loop VI) and G_{638} (stem loop I) are positioned in close proximity to the scissile phosphate [72]. Biochemical evidence suggests that A_{756} acts as the general acid and G_{638} as the general base during self-scission [73,74], similarly to the mechanism proposed for the hairpin ribozyme, wherein a guanosine and adenosine facilitate general acid-base catalysis (Table 1).

Glucosamine-6-Phosphate Synthase Ribozyme

The *glmS* ribozyme was discovered as a conserved motif located in the 5′ UTR of the *glmS* gene, encoding glutamine–fructose-6-phosphate transaminase, in many Gram-positive bacteria [75]. It is the only example of a metabolite-responsive self-cleaving ribozyme, utilizing glucosamine 6-phosphate (glcN6P) as a cofactor necessary for catalysis. It is also a riboswitch, regulating the expression of the *glmS* gene by a negative feedback mechanism whereby scission of the mRNA results in degradation of the message and a decrease in synthesis of the enzyme generating the glcN6P. Self-cleavage is completely dependent on the presence of amine-containing ligands, and the pK_a of the amine functionality impacts reactivity but not binding affinity [76].

The *glmS* ribozyme comprises three coaxial stacks (P1 stacks P3.1, P4 stacks P4.1, and P2.1), which are packed in a nearly parallel fashion (Figure 3E). The core of the ribozyme is doubly pseudoknotted (P2.1 and P2.2 are pseudoknots). P2.2 contains the scissile phosphate and helps to form the binding site for the glcN6P cofactor. P3 and P4 are not necessary for activity;

however, they enhance cleavage by providing structural stability [75,77]. Crystal structures of both pre- and postcleavage states showed no significant conformational change upon ligand binding [78]. The crystal structures revealed the location of a divalent metal, the metabolite binding pocket, and the active site, and provided strong evidence for the role of glcN6P in the catalytic mechanism. Both glcN6P [79,80] and the competitive inhibitor glc6P [78] are buried in the metabolite binding pocket, and both the sugar and phosphate of the cofactor are recognized in the pocket: the G_1 nucleobase stacks on the sugar ring, and N1 hydrogen bonds to the phosphate, which also coordinates a Mg^{2+} cation. The 1-hydroxyl of glc6P donates an H-bond to the *pro-R*p oxygen of the scissile phosphate A_{-1} and accepts a H-bond from N1 of G_{65} (Figure 3E; numbering follows that of the ribozyme used in the crystal structure from [78]). The 2-OH of glc6P forms a H-bond with the 5′-O of G_1 [78], whereas, in the presence of glcN6P, the amine moiety makes the interaction, making it a strong candidate for general acid during catalysis [79].

At the active site, G_{65} forms an irregular base pair with A_{-1}. Together, G_{39} and G_{65} position the scissile phosphate by binding its nonbridging oxygens. These interactions, along with the 2′-endo ribose pucker of A_{-1}, twist the RNA backbone into a nearly perfect in-line conformation. The nucleotides 5′ and 3′ of the scissile phosphate are unstacked and splayed apart. Overall, the active site is remarkably rigid, perhaps explaining why the *glmS* ribozyme is the only ribozyme besides the ribosome to be active in the crystallized form.

G_{40} and the metabolite are ideally positioned to serve as general base and acid, respectively, in catalysis (Figure 3E). Raman crystallography revealed the ionization states of the glcN6P cofactor and supports the role of G_{40} in tuning the pK_a of both the phosphate and amine of the ligand [81]. This is remarkable considering that the amine of free glcN6P is neutral. Thus, the positively charged amine is positioned to serve in proton transfer. The relation between the ionization state of the cofactor and the ribozyme activity supports the role of the cofactor in proton transfer [82]; however, the only evidence for the respective roles of G_{40} and the glcN6P cofactor in catalysis are their positions within the active site. Further analyses of this riboswitch-ribozyme will help define the details of its catalytic mechanism.

Twister Ribozyme

The twister ribozyme was discovered in 2013 through bioinformatics searches for conserved RNA structural motifs [83]. The secondary structure comprises three stems (P1, P2, and P4) joined by internal and terminal loops (L1, L2, and L4). There are two pseudoknots: PK2 is formed between L1 and L4, whereas PK1 is formed by L2 and L4 (Figure 3F; the numbering convention follows that of [83]). The ribozyme can exist in an extended format with additional stem loops P3 and P5 creating a three- or four-way junction at L2. In addition, the twister ribozyme can exist in three circularly permuted varieties (P1, P3, or P5). Twister ribozymes demonstrate robust cleavage kinetics both *in vitro* (k_{obs} >1 min^{-1} under physiological conditions) and *in vivo* [83]. Biochemical and crystallographic evidence supports the roles of ten conserved nucleotides at the active site.

The crystal structure of the *Oryza sativa* (Osa-1-4) P1-type twister ribozyme lacking P3 and P5 was solved to a 2.3 Å resolution [84]. The structure correlates well with that predicted by covariation and in-line probing analysis [83]. Helices P1, PK1(T2), P2, and PK2(T1) are coaxially stacked and P4 lies approximately parallel to the stack. The active site is located in the major groove of the PK2(T1)-P2 helix. G_{45} donates a H-bond to the *proR*-O of the scissile phosphate of A7 (in P1) and has been proposed to transfer the 2′ proton during catalysis [84]. Although there is no direct biochemical evidence, modeling based on the crystal structure points to a possible role of A_7 in the catalytic mechanism (Figure 3F) [84]. Another crystal structure of a P1-type twister identified in a metagenomic sequence revealed a Mg^{2+} ion near the scissile phosphate [85]. As in many other ribozyme active sites, the nucleotides flanking the scissile phosphate are splayed apart, promoting the in-line arrangement necessary for catalysis. The resolution of a divalent

cation along with the ordering and in-line arrangement of the U_6 nucleophile and A_7 leaving group are unique to this study and provide further elucidation of the factors contributing to the remarkable rates of catalysis by twister ribozymes.

Two additional crystal structures of type-P3 twister ribozymes from *O. sativa* and an environmental (metagenomic) sequence further suggest that a conserved adenosine is involved in stabilizing the negative charge on a nonbridging oxygen at the cleavage site, in addition to a guanosine activating the nucleophile [86]. The twister crystal structures suggest the utilization of a transition state stabilization strategy similar to the hairpin ribozyme. Remarkably, the source of protons for the 5′ oxyanion leaving group remains unknown (Table 1); however, crystallization of a transition state analog of the ribozyme may yet reveal a new active site rearrangement and clearly defined proton donor.

Mechanistic Conclusions

What have we learned so far? As Table 1 shows, the common theme in ribozyme self-scission is general acid-base catalysis. Ribozymes were originally thought to be metalloenzymes, in which the RNA serves to position catalytic Mg^{2+} ions to accelerate phosphoryl transfer [87,88]. The small self-cleaving ribozymes described here have evolved catalytic mechanisms mostly independent of metal ions and the origin of this mechanistic separation is unknown. A notable distinction between the two groups of phosphotransferases is that the self-cleavers act just once, whereas the larger ribozymes act twice (in case of self-splicing introns) or more (in case of the spliceosome and RNase P). Some of these small ribozymes represent the simplest evolutionary solution, as *in vitro* selections suggest [89], and general acid-base catalysis is perhaps the simpler mechanistic solution to RNA self-scission (see Outstanding Questions).

Biological Significance

Self-cleaving ribozymes are remarkably efficient enzymes, and we are continuing to discover their importance in biological systems. The biology of these common ribozymes remains one of the most unexplored areas of RNA research. The *glmS* ribozyme is unique in its role as a riboswitch controlling the flux of glcN6P in many Gram-positive bacteria. For the hairpin and VS ribozymes, each known instance is associated with a defined biological role in viral genome replication, although their true distribution may reach further than we currently understand. The HHR, HDV-like, and twister ribozyme families are widespread and found in diverse biological contexts, but only a few isolated occurrences have been studied for their particular influence on genetic controls [6,36].

The presence of self-cleaving ribozymes in intronic regions presents an exciting avenue of research with relevance to pre-mRNA processing and alternative splicing. Multiple HHRs are found in introns of a conserved set of genes in amniotes [32] and the ultraconserved HDV-like ribozyme mapping to the *CPEB3* gene in mammals is also located in an intron [4]. For the *CPEB3* and R2 retrotransposon-associated HDV-like ribozymes, reverse transcription-quantitative PCR (RT-qPCR) analyses demonstrate that the levels of cleaved product vary by tissue or life stage, respectively [4,5]. These observations suggest that the catalytic activity of these ribozymes is regulated, lending additional support to the idea that ribozymes are presenting an additional level of control for the expression of genes in which they reside. Interestingly, engineering self-cleaving ribozymes into introns or exons is a strategy used to understand co-transcriptional pre-mRNA processing [90]. These studies use a kinetic competition between splicing and ribozyme self-cleavage, the latter of which is disruptive to splicing [91] if ribozyme catalytic rates are ‘fast’ enough so as to interfere with spliceosome assembly [90].

In some natural cases, multiple ribozymes are found near each other in the same genomic locus [5,31,83], suggesting a cooperative influence on transcript processing or function. For example,

some eukaryotic HHRs that are found associated with **Penelope-like elements** (PLEs), a family of retrotransposons, display an organization suggestive of dimerization [92]. The dimeric form, containing two sites of self-cleavage, is possible when HHRs occur in tandem and has been shown to lead to a more stable active structure compared with monomeric species of the ribozyme [93]. By contrast, the discontinuous HHR present in the 3′ UTR of rodent *Clec2* genes is a single HHR in which invariant regions comprising the ribozyme core are separated by hundreds of nucleotides. The self-cleavage activity of this *Clec2* HHR removes the polyadenylation signal from the 3′ end of the mRNA, leading to a reduction in protein expression *in vivo* [37].

Very few known self-cleaving ribozymes are highly conserved among eukaryotic genomes. In rare instances, such as the *Clec2*-associated HHRs and the *CPEB3* HDV-like ribozymes, a single ribozyme sequence is conserved across multiple organisms [4,37], demonstrating that the self-scission activity was preserved through evolutionary lineages. By contrast, many instances of HHR, HDV-like, and twister ribozymes are found associated with mobile genetic elements and, thus, are not well conserved in terms of genetic loci or even sequence [5,92,94]. The extensive distribution of these ribozymes suggests they are common genomic features, perhaps distributed via (sub-)viral elements, retrotransposons, and other repeats, but now associated with multiple biological functions. While the field has gained a wealth of knowledge from studying independent examples of genetic elements harboring self-cleaving ribozymes, the biological significance of many other instances remains elusive.

The discovery of new self-cleaving ribozymes has transitioned from uncovering autocatalysis by single transcripts to high-throughput bioinformatic approaches to identifying conserved RNA structures. As the power of computational and high-throughput RNA structure probing methods continues to grow, undoubtedly new complex and intricate RNA motifs will be revealed, among them possibly new families of self-cleaving ribozymes. In fact, recent computational searches have uncovered structural variants of known ribozymes and discovered new conserved RNA motifs in bacterial genomes. Three new families of ribozymes have been validated for self-cleavage activity *in vitro*: twister sister, hatchet, and pistol [95]. These new ribozyme families provide the opportunity to gain insight into the biochemical capacity of structured RNAs and further understanding of the biological significance of self-cleaving ribozymes.

In vitro selections from genomic and synthetic DNA pools suggest that there are other motifs in nature capable of catalyzing self-scission and its reverse, ligation [4,89,96]. In addition, ribozyme catalysis can be studied in a *trans*-cleaving format, where the bisection of the secondary structure allows substrate recognition to regulate the rate of catalysis. The ease with which robust *trans*-cleaving ribozymes can be designed and constructed suggests that these intermolecular interactions also exist in nature. Similar to ribozymes, riboswitches are typically *cis*-acting, controlling transcription, translation, or stability of the proximal mRNA. Interestingly, an *S*-adenosyl methionine riboswitch element in the genome of *Listeria monocytogenes* behaves not only as a riboswitch in *cis*, but also as a regulatory ncRNA in *trans* [97]. This highlights the possibility that functional RNAs, such as ribozymes and riboswitches, can be responsible for performing multiple tasks. In this regard, engineering of natural ribozymes has provided additional insight.

Merging the ribozyme and riboswitch fields has created new tools to artificially control gene expression [98,99]. Aptazymes are engineered RNAs comprising both a ligand-binding domain and a ribozyme domain. They were first engineered as allosteric ribozymes via the fusion of an ATP aptamer and a HHR, whereby the sensing of ATP by the aptamer domain resulted in tuning of the HHR rate of catalysis [100]. The ability to adapt ribozymes into unnatural and unprecedented functional platforms attests to the versatility of these RNAs [101]. The functional

flexibility of ribozymes and the dynamic range in catalytic rates makes these RNAs versatile tools in the synthetic biologist toolbox. Perhaps some of the tricks we ask ribozymes to perform *in vitro* or *in vivo* are really characteristics that nature already uses but that remain undiscovered.

Concluding Remarks

In summary, the six families of self-cleaving ribozymes described here represent some of the smallest catalytic molecules known to biology. The intricate and elegant structures unique to each ribozyme family depict different means of accomplishing the same reaction. This is useful to synthetic biology, where ribozymes can be used as platforms conveying information about ligand recognition and molecular targeting. Equally exciting and consuming is the idea that there may be many more natural RNA structures capable of catalysis that are yet to be discovered. The vast distribution of some of the ribozyme families presented here leads to many intriguing questions regarding their biological relevance.

Outstanding Questions

What are the mechanisms of transition-state (or intermediate) stabilization during ribozyme catalysis for all known self-cleaving ribozymes?

What are the strategies to shift the pK_as of active site groups involved in catalysis?

Are there natural *trans*-cleaving ribozymes?

Are there natural aptazymes?

What are the effects of mammalian self-cleaving ribozymes on their hosts?

References

1. Lai, M.M. (1995) The molecular biology of hepatitis delta virus. *Annu. Rev. Biochem.* 64, 259–286
2. Taylor, J.M. (1999) Hepatitis delta virus. *Intervirology* 42, 173–178
3. Wu, H.N. *et al.* (1989) Human hepatitis-delta virus-RNA subfragments contain an autocleavage activity. *Proc. Natl. Acad. Sci. U.S.A.* 86, 1831–1835
4. Salehi-Ashtiani, K. *et al.* (2006) A genomewide search for ribozymes reveals an HDV-like sequence in the human CPEB3 gene. *Science* 313, 1788–1792
5. Webb, C.H. *et al.* (2009) Widespread occurrence of self-cleaving ribozymes. *Science* 326, 953
6. Ruminski, D.J. *et al.* (2011) Processing and translation initiation of non-long terminal repeat retrotransposons by hepatitis delta virus (HDV)-like self-cleaving ribozymes. *J. Biol. Chem.* 286, 41286–41295
7. Eickbush, D.G. and Eickbush, T.H. (2010) R2 retrotransposons encode a self-cleaving ribozyme for processing from an rRNA cotranscript. *Mol. Cell. Biol.* 30, 3142–3150
8. Sanchez-Luque, F.J. *et al.* (2011) Identification of an hepatitis delta virus-like ribozyme at the mRNA 5′-end of the L1Tc retrotransposon from *Trypanosoma cruzi*. *Nucleic Acids Res.* 39, 8065–8077
9. Bibillo, A. and Eickbush, T.H. (2002) The reverse transcriptase of the R2 non-LTR retrotransposon: continuous synthesis of cDNA on non-continuous RNA templates. *J. Mol. Biol.* 316, 459–473
10. Bibillo, A. and Eickbush, T.H. (2004) End-to-end template jumping by the reverse transcriptase encoded by the R2 retrotransposon. *J. Biol. Chem.* 279, 14945–14953
11. Vogler, C. *et al.* (2009) CPEB3 is associated with human episodic memory. *Front. Behav. Neurosci.* 3, 4
12. Smith, J.B. and Dinter-Gottlieb, G. (1991) Antigenomic Hepatitis delta virus ribozymes self-cleave in 18 M formamide. *Nucleic Acids Res.* 19, 1285–1289
13. Duhamel, J. *et al.* (1996) Secondary structure content of the HDV ribozyme in 95% formamide. *Nucleic Acids Res.* 24, 3911–3917
14. Ferre-D'Amare, A.R. *et al.* (1998) Crystal structure of a hepatitis delta virus ribozyme. *Nature* 395, 567–574
15. Ke, A. *et al.* (2004) A conformational switch controls hepatitis delta virus ribozyme catalysis. *Nature* 429, 201–205
16. Chen, J.H. *et al.* (2010) A 1.9 A crystal structure of the HDV ribozyme precleavage suggests both Lewis acid and general acid mechanisms contribute to phosphodiester cleavage. *Biochemistry* 49, 6508–6518
17. Gong, B. *et al.* (2009) Competition between Co(NH(3)(6)3$^+$ and inner sphere Mg2$^+$ ions in the HDV ribozyme. *Biochemistry* 48, 11961–11970
18. Golden, B.L. (2011) Two distinct catalytic strategies in the hepatitis delta virus ribozyme cleavage reaction. *Biochemistry* 50, 9424–9433
19. Das, S.R. and Piccirilli, J.A. (2005) General acid catalysis by the hepatitis delta virus ribozyme. *Nat. Chem. Biol.* 1, 45–52
20. Thaplyal, P. *et al.* (2015) Inverse thio effects in the hepatitis delta virus ribozyme reveal that the reaction pathway is controlled by metal ion charge density. *Biochemistry* 54, 2160–2175
21. Perrotta, A.T. and Been, M.D. (2006) HDV ribozyme activity in monovalent cations. *Biochemistry* 45, 11357–11365
22. Luptak, A. *et al.* (2001) Direct p*K*(a) measurement of the active-site cytosine in a genomic hepatitis delta virus ribozyme. *J. Am. Chem. Soc.* 123, 8447–8452
23. Gong, B. *et al.* (2007) Direct measurement of a p*K*(a) near neutrality for the catalytic cytosine in the genomic HDV ribozyme using Raman crystallography. *J. Am. Chem. Soc.* 129, 13335–13342
24. Prody, G.A. *et al.* (1986) Autolytic processing of dimeric plant virus satellite RNA. *Science* 231, 1577–1580
25. Forster, A.C. and Symons, R.H. (1987) Self-cleavage of virusoid RNA is performed by the proposed 55-nucleotide active-site. *Cell* 50, 9–16
26. Forster, A.C. and Symons, R.H. (1987) Self-cleavage of plus and minus RNAs of a virusoid and a structural model for the active sites. *Cell* 49, 211–220
27. Epstein, L.M. and Gall, J.G. (1987) Transcripts of newt satellite DNA self-cleave in vitro. *Cold Spring Harb. Symp. Quant. Biol.* 52, 261–265
28. Rojas, A.A. *et al.* (2000) Hammerhead-mediated processing of satellite pDo500 family transcripts from *Dolichopoda* cave crickets. *Nucleic Acids Res.* 28, 4037–4043
29. Ferbeyre, G. *et al.* (1998) Schistosome satellite DNA encodes active hammerhead ribozymes. *Mol. Cell. Biol.* 18, 3880–3888
30. Laha, T. *et al.* (2000) Sjalpha elements, short interspersed element-like retroposons bearing a hammerhead ribozyme motif from the genome of the oriental blood fluke Schistosoma japonicum. *Biochim. Biophys. Acta* 1492, 477–482
31. de la Pena, M. and Garcia-Robles, I. (2010) Ubiquitous presence of the hammerhead ribozyme motif along the tree of life. *RNA* 16, 1943–1950
32. de la Pena, M. and Garcia-Robles, I. (2010) Intronic hammerhead ribozymes are ultraconserved in the human genome. *EMBO Rep.* 11, 711–716
33. Perreault, J. *et al.* (2011) Identification of hammerhead ribozymes in all domains of life reveals novel structural variations. *PLoS Comput. Biol.* 7, e1002031
34. Jimenez, R.M. *et al.* (2011) Structure-based search reveals hammerhead ribozymes in the human microbiome. *J. Biol. Chem.* 286, 7737–7743
35. Seehafer, C. *et al.* (2011) From alpaca to zebrafish: hammerhead ribozymes wherever you look. *RNA* 17, 21–26
36. Garcia-Robles, I. *et al.* (2012) Intronic hammerhead ribozymes in mRNA biogenesis. *Biol. Chem.* 393, 1317–1326

37. Martick, M. *et al.* (2008) A discontinuous hammerhead ribozyme embedded in a mammalian messenger RNA. *Nature* 454, 899–902
38. Pley, H.W. *et al.* (1994) Three-dimensional structure of a hammerhead ribozyme. *Nature* 372, 68–74
39. Scott, W.G. *et al.* (1996) Capturing the structure of a catalytic RNA intermediate: the hammerhead ribozyme. *Science* 274, 2065–2069
40. Khvorova, A. *et al.* (2003) Sequence elements outside the hammerhead ribozyme catalytic core enable intracellular activity. *Nat. Struct. Biol.* 10, 708–712
41. De la Pena, M. *et al.* (2003) Peripheral regions of natural hammerhead ribozymes greatly increase their self-cleavage activity. *EMBO J.* 22, 5561–5570
42. Martick, M. and Scott, W.G. (2006) Tertiary contacts distant from the active site prime a ribozyme for catalysis. *Cell* 126, 309–320
43. Ferre-D'Amare, A.R. and Scott, W.G. (2010) Small self-cleaving ribozymes. *Cold Spring Harb. Perspect. Biol.* 2, a003574
44. Anderson, M. *et al.* (2013) Active-site monovalent cations revealed in a 1.55-A-resolution hammerhead ribozyme structure. *J. Mol. Biol.* 425, 3790–3798
45. Han, J. and Burke, J.M. (2005) Model for general acid-base catalysis by the hammerhead ribozyme: pH-activity relationships of G8 and G12 variants at the putative active site. *Biochemistry* 44, 7864–7870
46. Roychowdhury-Saha, M. and Burke, D.H. (2007) Distinct reaction pathway promoted by non-divalent-metal cations in a tertiary stabilized hammerhead ribozyme. *RNA* 13, 841–848
47. Chi, Y.I. *et al.* (2008) Capturing hammerhead ribozyme structures in action by modulating general base catalysis. *PLoS Biol.* 6, 2060–2068
48. Martick, M. *et al.* (2008) Solvent structure and hammerhead ribozyme catalysis. *Chem. Biol.* 15, 332–342
49. Rubino, L. *et al.* (1990) Nucleotide sequence and structural analysis of two satellite RNAs associated with chicory yellow mottle virus. *J. Gen. Virol.* 71, 1897–1903
50. Kaper, J.M. *et al.* (1988) Nucleotide sequence predicts circularity and self-cleavage of 300-ribonucleotide satellite of arabis mosaic virus. *Biochem. Biophys. Res. Commun.* 154, 318–325
51. Grum-Tokars, V. *et al.* (2003) Crystallization and X-ray diffraction analysis of an all-RNA U39C mutant of the minimal hairpin ribozyme. *Acta Crystallogr. D: Biol. Crystallogr.* 59, 142–145
52. Rupert, P.B. and Ferre-D'Amare, A.R. (2001) Crystal structure of a hairpin ribozyme-inhibitor complex with implications for catalysis. *Nature* 410, 780–786
53. Rupert, P.B. *et al.* (2002) Transition state stabilization by a catalytic RNA. *Science* 298, 1421–1424
54. Tan, E. *et al.* (2003) A four-way junction accelerates hairpin ribozyme folding via a discrete intermediate. *Proc. Natl. Acad. Sci. U.S.A.* 100, 9308–9313
55. Nahas, M.K. *et al.* (2004) Observation of internal cleavage and ligation reactions of a ribozyme. *Nat. Struct. Mol. Biol.* 11, 1107–1113
56. Kuzmin, Y.I. *et al.* (2004) Role of an active site guanine in hairpin ribozyme catalysis probed by exogenous nucleobase rescue. *J. Mol. Biol.* 340, 233–251
57. Kuzmin, Y.I. *et al.* (2005) Role of an active site adenine in hairpin ribozyme catalysis. *J. Mol. Biol.* 349, 989–1010
58. Wilson, T.J. *et al.* (2006) Nucleobase catalysis in the hairpin ribozyme. *RNA* 12, 980–987
59. Pinard, R. *et al.* (2001) Functional involvement of G8 in the hairpin ribozyme cleavage mechanism. *EMBO J.* 20, 6434–6442
60. Collins, R.A. (2002) The *Neurospora* Varkud satellite ribozyme. *Biochem. Soc. Trans.* 30, 1122–1126
61. Bouchard, P. and Legault, P. (2014) A remarkably stable kissing-loop interaction defines substrate recognition by the *Neurospora* Varkud Satellite ribozyme. *RNA* 20, 1451–1464
62. Beattie, T.L. *et al.* (1995) A secondary-structure model for the self-cleaving region of *Neurospora* VS RNA. *Proc. Natl. Acad. Sci. U.S.A.* 92, 4686–4690
63. Rastogi, T. *et al.* (1996) A long-range pseudoknot is required for activity of the *Neurospora* VS ribozyme. *EMBO J.* 15, 2820–2825
64. Andersen, A.A. and Collins, R.A. (2000) Rearrangement of a stable RNA secondary structure during VS ribozyme catalysis. *Mol. Cell* 5, 469–478
65. Andersen, A.A. and Collins, R.A. (2001) Intramolecular secondary structure rearrangement by the kissing interaction of the *Neurospora* VS ribozyme. *Proc. Natl. Acad. Sci. U.S.A.* 98, 7730–7735
66. Flinders, J. and Dieckmann, T. (2001) A pH controlled conformational switch in the cleavage site of the VS ribozyme substrate RNA. *J. Mol. Biol.* 308, 665–679
67. Hiley, S.L. and Collins, R.A. (2001) Rapid formation of a solvent-inaccessible core in the *Neurospora* Varkud satellite ribozyme. *EMBO J.* 20, 5461–5469
68. Hiley, S.L. *et al.* (2002) 4-thio-U cross-linking identifies the active site of the VS ribozyme. *EMBO J.* 21, 4691–4698
69. Bouchard, P. and Legault, P. (2014) Structural insights into substrate recognition by the *Neurospora* Varkud satellite ribozyme: importance of U-turns at the kissing-loop junction. *Biochemistry* 53, 258–269
70. Michiels, P.J.A. *et al.* (2000) Structure of the ribozyme substrate hairpin of *Neurospora* VS RNA: a close look at the cleavage site. *RNA* 6, 1821–1832
71. Hoffmann, B. *et al.* (2003) NMR structure of the active conformation of the Varkud satellite ribozyme cleavage site. *Proc. Natl. Acad. Sci. U.S.A.* 100, 7003–7008
72. Lipfert, J. *et al.* (2008) The complete VS ribozyme in solution studied by small-angle X-ray scattering. *Structure* 16, 1357–1367
73. Wilson, T.J. *et al.* (2007) A guanine nucleobase important for catalysis by the VS ribozyme. *EMBO J.* 26, 2489–2500
74. Wilson, T.J. *et al.* (2010) Nucleobase-mediated general acid-base catalysis in the Varkud satellite ribozyme. *Proc. Natl. Acad. Sci. U.S.A.* 107, 11751–11756
75. Winkler, W.C. *et al.* (2004) Control of gene expression by a natural metabolite-responsive ribozyme. *Nature* 428, 281–286
76. McCarthy, T.J. *et al.* (2005) Ligand requirements for glmS ribozyme self-cleavage. *Chem. Biol.* 12, 1221–1226
77. Roth, A. *et al.* (2006) Characteristics of the glmS ribozyme suggest only structural roles for divalent metal ions. *RNA* 12, 607–619
78. Klein, D.J. and Ferre-D'Amare, A.R. (2006) Structural basis of glmS ribozyme activation by glucosamine-6-phosphate. *Science* 313, 1752–1756
79. Cochrane, J.C. *et al.* (2007) Structural investigation of the glmS ribozyme bound to Its catalytic cofactor. *Chem. Biol.* 14, 97–105
80. Cochrane, J.C. *et al.* (2009) Structural and chemical basis for glucosamine 6-phosphate binding and activation of the glmS ribozyme. *Biochemistry* 48, 3239–3246
81. Gong, B. *et al.* (2011) The glmS ribozyme tunes the catalytically critical p*K*(a) of its coenzyme glucosamine-6-phosphate. *J. Am. Chem. Soc.* 133, 14188–14191
82. Viladoms, J. and Fedor, M.J. (2012) The glmS ribozyme cofactor is a general acid-base catalyst. *J. Am. Chem. Soc.* 134, 19043–19049
83. Roth, A. *et al.* (2014) A widespread self-cleaving ribozyme class is revealed by bioinformatics. *Nat. Chem. Biol.* 10, 56–60
84. Liu, Y. *et al.* (2014) Crystal structure and mechanistic investigation of the twister ribozyme. *Nat. Chem. Biol.* 10, 739–744
85. Ren, A.M. *et al.* (2014) In-line alignment and Mg^{2+} coordination at the cleavage site of the env22 twister ribozyme. *Nat. Commun.* 5, 5534
86. Eiler, D. *et al.* (2014) Structural basis for the fast self-cleavage reaction catalyzed by the twister ribozyme. *Proc. Natl. Acad. Sci. U.S.A.* 111, 13028–13033
87. Pyle, A.M. (1993) Ribozymes: a distinct class of metalloenzymes. *Science* 261, 709–714
88. Yarus, M. (1993) How many catalytic RNAs? Ions and the Cheshire cat conjecture. *FASEB J.* 7, 31–39

89. Salehi-Ashtiani, K. and Szostak, J.W. (2001) In vitro evolution suggests multiple origins for the hammerhead ribozyme. *Nature* 414, 82–84

90. Fong, N. *et al.* (2009) Fast ribozyme cleavage releases transcripts from RNA polymerase II and aborts co-transcriptional pre-mRNA processing. *Nat. Struct. Mol. Biol.* 16, 916–922

91. Lacadie, S.A. *et al.* (2006) In vivo commitment to yeast cotranscriptional splicing is sensitive to transcription elongation mutants. *Genes Dev.* 20, 2055–2066

92. Cervera, A. and De la Pena, M. (2014) Eukaryotic penelope-like retroelements encode hammerhead ribozyme motifs. *Mol. Biol. Evol.* 31, 2941–2947

93. Forster, A.C. *et al.* (1988) Self-cleaving viroid and newt RNAs may only be active as dimers. *Nature* 334, 265–267

94. Hammann, C. *et al.* (2012) The ubiquitous hammerhead ribozyme. *RNA* 18, 871–885

95. Weinberg, Z. *et al.* (2015) New classes of self-cleaving ribozymes revealed by comparative genomics analysis. *Nat. Chem. Biol.* 11, 606–610

96. Tang, J. and Breaker, R.R. (2000) Structural diversity of self-cleaving ribozymes. *Proc. Natl. Acad. Sci. U.S.A.* 97, 5784–5789

97. Loh, E. *et al.* (2009) A trans-acting riboswitch controls expression of the virulence regulator PrfA in *Listeria monocytogenes*. *Cell* 139, 770–779

98. Vinkenborg, J.L. *et al.* (2011) Aptamers for allosteric regulation. *Nat. Chem. Biol.* 7, 519–527

99. Famulok, M. *et al.* (2007) Functional aptamers and aptazymes in biotechnology, diagnostics, and therapy. *Chem. Rev.* 107, 3715–3743

100. Tang, J. and Breaker, R.R. (1997) Rational design of allosteric ribozymes. *Chem. Biol.* 4, 453–459

101. Carothers, J.M. *et al.* (2011) Model-driven engineering of RNA devices to quantitatively program gene expression. *Science* 334, 1716–1719

102. Riccitelli, N.J. and Luptak, A. (2010) Computational discovery of folded RNA domains in genomes and in vitro selected libraries. *Methods* 52, 133–140